مجلة كلية التربية الاساسية
كلية التربية الاساسية – الجامعة المستنصرية
Journal of the College of Basic Education Vol.31 (NO. 129) 2025, pp. 130-147

Repairing Rabbit Femur Bone Defects with Graphene Oxide Scaffolds and Gold Nanoparticles

Wahab Basim Mahdi[1], Hajer Tounsi Guermazi [2]
[1] Department of Physics ,*college of science, Mustansiriyah University, Baghdad, Iraq*
[2] Department of Physics, *Faculty of Science of Sfax, Sfax University, Tunisia*
07750777599
92019819

Abstract :

*Background :*The byproduct of graphite oxidation is graphene oxide, which offers a tremendous chance to advance the field of regenerative medicine significantly. Because of graphene oxide's favorable qualities— Because of its adaptable mechanical qualities, biocompatibility, and degradability. Objective: This research aims to employ laser rays to ablate the graphite surface and prepare graphene oxide with excellent mechanical properties that contribute to the treatment of rabbit bone injuries, regeneration of damaged bone tissue and osteogenic differentiation .Methods: In this work, the xeno bony scaffolds implantation were prepared in two parts physically: were effectively generated graphene oxide(GO) by using laser ablation technique .Lasing pulse duration(1064 nm) with laser energy (300 mJ), after that, gold nanoparticles(AuNPs) prepared previous were loaded on the graphene oxide surface by using chips method. The structure and morphology of the composite (GO: AuNPs) were analyzed through Fourier Transform Infrared Spectroscopy (FTIR) and X-Ray Diffraction (XRD) to assess its chemical composition and crystalline structure. Raman spectroscopy and transmission electron microscopy (TEM) were then used to examine the edge/crystalline orientations and stacking orders of graphene oxide.: In this section, the technique of preparing a pin template to anchor the scaffold implantation into the rabbits' stimulated femoral bone fractions is described. A combination made of Graphene oxide and gold nanoparticles were utilized to create the xeno bony scaffold. Results. The histological results in vivo of the site treated with (GO: AuNP) scaffolds, harvested at 1st week after grafting showed bone mineralization and abundant new bone formation without any sign of inflammation in treatment group. Moreover, the in vitro tests demonstrate that the (GO: AuNP) scaffolds greatly enhance osteoblast adhesion cells as well as growth. Conclusion :the application of graphene oxide (GO) enhanced calcium and protein adsorption, enzyme resistance, and physical strength.

Keywords: graphene oxide ,gold nanoparticles, xeno bony scaffold, Laser ablation, Femur Bone

Note: The research is taken from a doctoral thesis.

Introduction

A fiber consisting of carbon atoms firmly packed into a two-dimensional (2D) honeycomb lattice is called graphene [1]. With two different types of bonds between the atoms [1], The combination of graphite with the suffix -ene, which was previously employed in the nomenclature and terminology of polycyclic aromatic hydrocarbons, is where the term "graphene" originates [2] . In recent decades, graphene, has attracted tremendous attention, Its adaptable qualities include high surface area, electrical and mechanical capabilities, charge carrier mobility, and thermal conductivity [3]has been used widely in catalysts, super capacitors, transparent electrodes, electrochemical detection, biomedicine [4] Graphene oxide is one of graphene's many compounds. GO has proven to be quite useful in situations including water since it overcomes hydrophobicity, a drawback of graphene that prevents it from being used in biomedicine. The number of proof-of-concept studies examining GO's suitability for application in biomedicine is rising.[5] Excellent characteristics of graphene oxide include a high aspect ratio and good conductivity .exceptional electrical insulating qualities, a distinct graphitized planar structure, and excellent mechanical strength [6]. Graphene oxide has been used in numerous studies to create scaffolds for bone tissue engineering and use them to cure bone defects. Because of its excellent mechanical characteristics, degradability, and biocompatibility[7].GO is the most extensively utilized material. GO's unique surface structure and profusion of functional groups gave it numerous exceptional qualities, including strong mechanical strength, good hydrophobicity, and antibacterial capabilities [8]. Furthermore, numerous investigations have shown that GO have a potent ability to induce osteogenesis. According to some research, GO can increase cytoskeletal stress, which in turn can stimulate osteogenic differentiation [9]. Moreover, GO's potent protein adsorption ability can draw the nutrients needed for cell growth to the material surface, improving the living conditions[10]. More significantly, a variety of oxygen-containing active groups, including epoxy, carboxyl, and hydroxyl groups, make it easier to modify the GO surface by adding bioactive components to enhance its characteristics. Numerous techniques have been used to enhance the capacity for bone healing. such as mixing some bioactive nanoparticles, including gold nanoparticles (AuNPs), with GO to create composites [11]These nanoparticles have the ability to control cell activity, promote bone cell proliferation, strengthen scaffolds mechanically, and help the material fuse with the surrounding bone tissue. This tactic can increase the ability to heal bones [12].

In this study, we prepare GO chemically with laser Nd:YAG by Laser ablation, and blended with Au NPs to create porous composite scaffolds (laser GO :AuNPs). After that, we applied scaffold (GO: AuNPs) composite on bone tissue regeneration in rabbit. TEM, mechanical testing, and antibacterial studies were used to investigate the physical and chemical properties of the scaffolds. Also.

Materials And Methods

Materials

Table 1. Materials used in study

Items	Materials	Chemical formula	Specification	company
1	Graphite powder	G	8mg	Sigma
2	Polyvinylpyrrolidone	PVP	23mg	Sigma
3	Acetone	CH_3COCH_3	80ml	Sigma
4	Chloroauric acid	$HAuCl_4$	1 mg	Sigma

Methods

Preparation of the physical part

1. The production of graphene oxide (GO) nanoparticles via laser ablation technique

The graphene oxide disc was prepared by mixing 2 ml of graphite with 4 mg of Polyvinylpyrrolidone (PVP) powder, which was then dissolved in approximately 10 ml of deionized water under magnetic stirring for 10 minutes. The mixture was allowed to dry for two days. Following the drying process, the disc sample was cut into several 5 mm diameter pieces for the purpose of laser ablation on its surface, as shown in figure 1. The graphite target, submerged in water, was ablated using a Q-switched pulsed Nd:YAG laser (SureLite Continuum) operating at a wavelength of 1064 nm, with a pulse repetition rate of 2 Hz and a pulse duration of 0.5 ms (laser beam spot size = 2.06 mm). A 5 mm diameter graphite sample was positioned at the bottom of a glass vessel containing 20 milliliters of estimation. The laser energy was set to 300 mJ for 400 pulses. The experimental setup for the preparation process is depicted in Figure (2). To achieve consistent ablation, the target was continually rotated throughout the ablation procedure. On the surface of the sample, a layer of oxidized graphene oxide was. produced.

مجلة كلية التربية الاساسية
كلية التربية الاساسية – الجامعة المستنصرية
Journal of the College of Basic Education Vol.31 (NO. 129) 2025, pp. 130-147

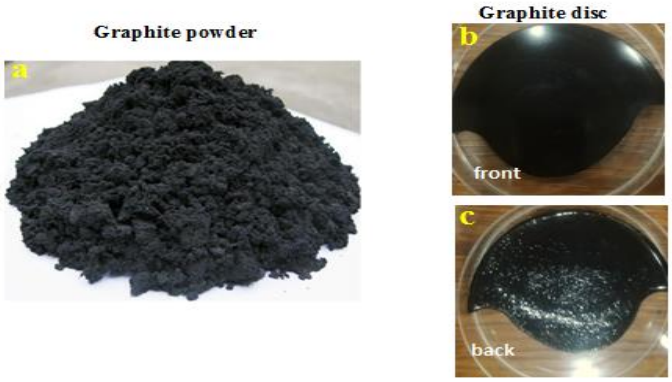

Figure 1: (a) Graphite powder, (b) front graphite disc and (c) back graphite disc

Figure 2: Creation of graphene oxide (GO) via laser ablation from graphite

2. Synthesis of gold nanoparticles

With a few adjustments, the Frens/Turkevich method was used to synthesize gold nanoparticles. A round-bottom flask (250 ml) with a magnetic stirring bar was used to vigorously stir a 100 ml solution of gold salt ($HAuCl_4$) to a boil at 100 °C. After that, sodium citrate solution was added. The molar ratio (MR) of NaCl to $HAuCl_4$ was the primary variable that was controlled to generate the right particle size. Depending on the MR, the resultant reaction mixture refluxed for an extra 20 minutes. As gold nanoparticles were formed, the fluid in the flask's hue shifted from colorless to gray, purple, and ultimately ruby red[13].

3.The preparation of GO :AuNP nanocomposites

Gold nanoparticles with Laser graphene oxide (GO) has been used target as shown in the figure(3) .The GO disc has been divided into several tiny pieces, each having a diameter of 5 mm and a thickness of 3 mm. By pushing the gold nanoparticle chips into an appropriate hole created on the GO target surface, the chips of the gold nanoparticles have been statically attached to the target

surface; initially, insert one AuNPs chip on the target surface. Two AuNPs chips are added to the target surface in the second phase, making a total of two gold chips. The last gold chip is added in the third step, making a total of three gold chips. Polishing the target's two faces after each deposition (sputter) procedure is crucial.

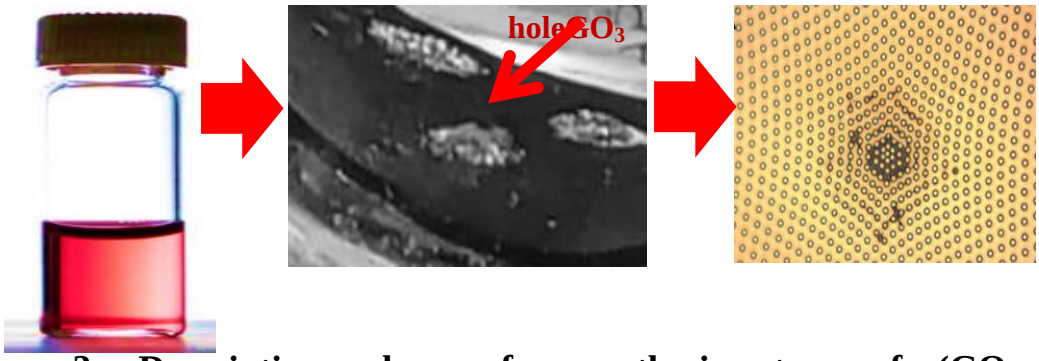

Figure 3: Descriptive scheme for synthesis steps of (GO: AuNPs)nanocomposites.

Preparation of the biological part

1. Setting Up a Pin Template

In this section, the method of creating a pin template to secure the implantation of the (GO: AuNPs) scaffold within the rabbits' stimulated femoral bone fractions is described. The required diameter and length, or around 7.5 and 2.5 cm, respectively - are measured as part of the procedure. Next, as indicated in the figure (4), sharpen the pin tips so that one side is sharper than the other, from both directions. Since animals are owned by Health Ministry and the NCDCR.

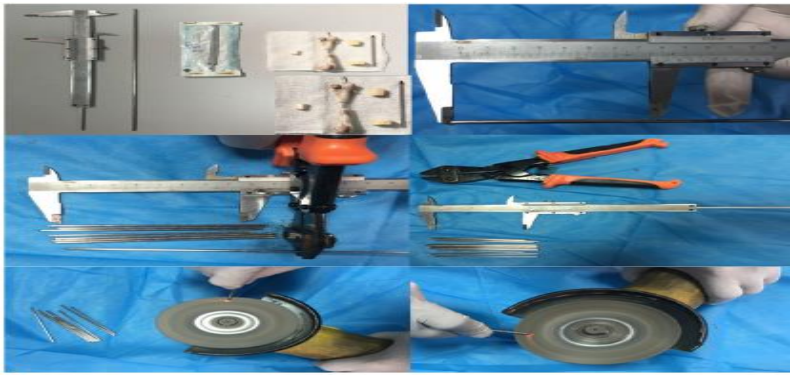

Figure 4 : The procedure that served as a pin template to secure the implantation of the corn scaffold that is within the rabbits' stimulated femoral bone sections.

National Center for Drug Control and Research, it is imperative to ensure that the experiment is conducted flawlessly. Before the procedure, the gathered rabbits were kept for seven days in particular cages(In experiments like these, it's essential to control as many variables as possible, such as the environment in which the animals are kept. Keeping the rabbits in these cages for seven days might help them acclimate to the environment, reduce stress, and ensure that the results of the experiment are as reliable as possible) shown in figures (5) and Table 2.

Figure 5 : The gathered bunnies were kept in designated cages.

Table 2. Adults' bone composition (%)

Calcium	*34.8*
Phosphoru s	*15.2*
Sodium	*0.9*
Magnesium	*0.72*
Potassium	*0.03*
Carbonates	*7.4*
Fluorine	*0.03*
Chlorine	*0.13*
Pyrophosphates	*0.07*
Other elements	*0.04*

Before the procedure, all of the animals were given an antiparasitic medication to prevent parasites both internal and external, use Ivermectin (0.1 mg/kg). Following surgery, the transverse fracture was created to remove roughly 1 centimeter of length at the femoral bone's mid-shift. Connectively. Approximately twenty rabbits were used in this experiment after The breach in the femur was filled with a scaffold implantation of an appropriate size (GO:

AuNPs) that was secured "The use of intramedullary pins as tools for internal fixation." Before a procedure, all tools, linens, and equipment were autoclaved for 30 minutes at 121 degrees Celsius and 20 bars (see figure 6).

Figure 6: autoclaved for 30 minutes at 121 degrees Celsius..

Following fracture surgery, the treatment groups received a single continuous diode laser dosage light at four points on the femur bone's lateral aspect, specifically on the sites of a xeno bone implantation. A control groups, on the other hand, were released for normal fracture healing without exposure to laser light. The exposure schedule was 5 minutes every 72 hours for 14 days after the procedure; the laser's dosage was 148.4 J/cm^2 energy per unit area at an 850 nm wavelength. Figure (7) illustrates how the appropriate quantity of antibiotics and anesthesia was determined by weighing each rabbit in a separate animal balance.

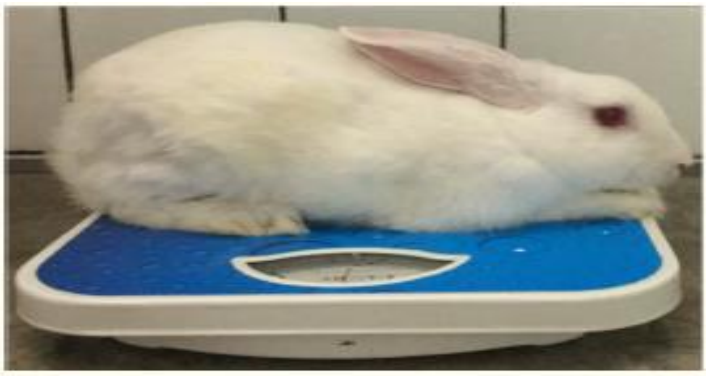

Figure 7:Balancing the weight of each rabbit individually for the benefit of the animals

Stages Prior to Surgery and Anesthesia Procedures

The surgical field, or the hip joint to the stifle joint, was prepared for a high-aseptic surgical procedure by shaving, cutting, then using tap water and soap to clean. The region was and then disinfected with 70% prepared alcohol figure

(8). The surgical toolkit, adhesive materials, and electrical New Zealand, laser apparatus, curtains, gowns, and gloves for surgery were all presented as necessary equipment for the procedure. Before the procedure, the rabbits were denied food and drink for 12 hours. A combination of intramuscular injections of 5% ketamine hydrochloride (25 mg/kg), 0.5 cc lidocaine, and 2% xylazine hydrochloride (17.5 mg/kg) was used to achieve general anesthesia. The following formula was used to calculate the anesthetic and antibiotic doses: dose is equal to the animal's weight times the drug's dosage rate.
dose = animals weight × dose rate constration of drug

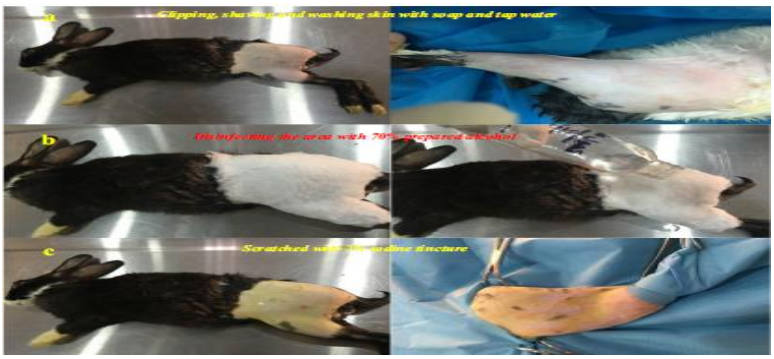

Figure 8: The sequential preparation steps of animal for the operation
Procedure for Surgery

After being put to sleep, the animals were placed in lateral recumbency, with sterile drapes covering their entire body except for the surgical field, which was wrapped in gauze soaked in alcohol and then scraped using (2%) tincture of iodine. A (4-cm) surgical incision was created from the great trochanter to the lateral side of the patella on the thigh's lateral surface. The femur bone's mid-shift was seen via the incision, which was made after the bleeding was regularly stopped, the subcutaneous tissue was dissected, the fascia lata was removed, and the vastus lateralis and biceps femoris muscles were bluntly separated.
The muscles and fascia lata were sutured using a simple continuous pattern using (2/0) chromic catgut each alone, the skin was closed using a simple interrupted pattern using 2/0 no absorbable silk materials, and the pins were introduced using the retrograde pin choke method (figure 9). Powdered penicillin was used as a topical antibiotic. After the surgery, radiographic imaging was used to verify the exact positioning of the intramedullary pins and the xeno bone implantation. Any extra pin material should be trimmed with a pin cutter.

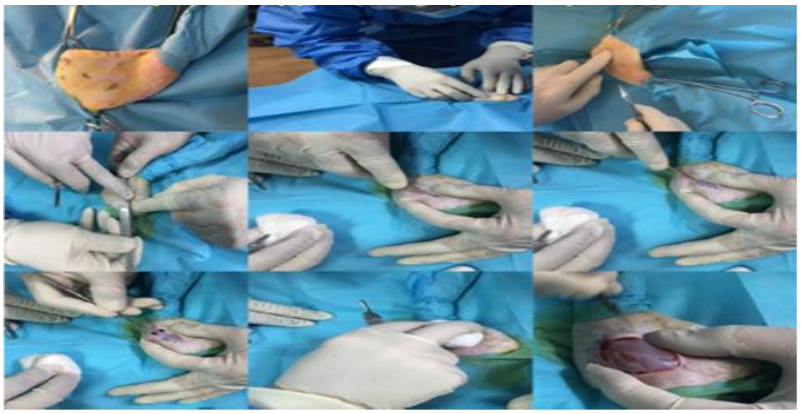

Figure 9: Procedures for intramedullary pinning the bone device with the two femoral

recipient fragments in order to perform surgical internal fixing

After Surgery Care

After the procedure, the animal was kept under observation until it regained consciousness and went back to the animal house.

• Every day, any anomalies such as bleeding, dehiscence of stitches, or abscesses in stitches were examined at the surgical site.

• As systemic antibiotics, intramuscular injections of penicillin and streptomycin (10 mg/kg) b.w. for streptomycin and (1000 IU/kg) b.w. for penicillin,were administered for three to five days following surgery.

• Removing the sutures 7-9 days after the procedure

Radiological assessment

All groups underwent radiographic evaluations on day 0 and at the conclusion of the first, second, third, fourth, and fifth week following surgery. Following the administration of light anesthetic or a sedative to relax the animals, a radiological examination was performed in two views: the medio-lateral and the anterior-posterior. The X-ray machine specifications were as follows .The dimensions of the X-ray film were 10 × 12 cm^2 or 14 × 17 inches, with 6–8 views per film. The exposure factors were energy (47 kV), current (2.20 mAS), and focusing distance (F.F.D. = 30 cm). automatic processor (XP400 processing machine) processed the (X-ray) movies in the dimly lit space. In order to save all modifications, the photos were lastly inspected using the eliminator

Histopathological Analysis

The Reason Behind Histology Procedures The goal of histology is to identify the most significant histological changes occurring along with the rate, amount, and degree of newly created bone as well as the degree of bone gap repair. At two, six, and twelve weeks following surgery Ten rabbits for each

group and five for each session, respectively., histological assessment was carried out. The intramedullary pins were taken out once the necessary amount of time had passed, and the animals were then scarified with a strong anesthetic. After the femur bone was removed, the muscles and soft tissues such as the skin were dissected.

Results and Discussion

XRD Analysis for laser ablation graphene oxide(GO)

One way to make graphene oxide is by oxidizing graphite using potent oxidants. In this work, the hexagonal lattice structure is preserved by graphene oxide [14]. Investigations by means of (X-ray diffraction, or XRD)) were used study the crystal structure of the laser ablation graphene oxide. The XRD patterns for are displayed in figure (10) GO has a distinct characteristics of carbon peak (001) appeared at 2ɵ = 10.90 and a broad diffraction new peak (002) appears at 2ɵ = 24.9 [15] . owing to the existence of carboxyl, epoxy and groups of hydroxyls, with d-spacing 8.19 Å. Oxygen groups in materials made of graphene are advantageous of a number of uses, particularly in bone tissue. [16]

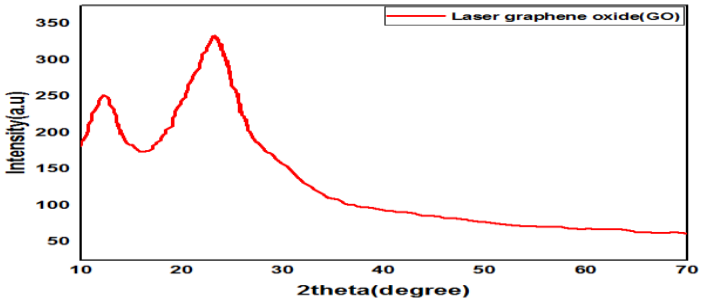

Figure 10: XRD patterns for Laser graphene oxide(GO)

FTIR for Laser graphene oxide (GO)

FTIR spectra of GO figure (11) showed various functional groups and the characteristic absorption bands were summarized in table (3).The CO–H stretching vibrations of a hydroxyl group, which show that the structure contains OH and/or COOH functional groups, created a very strong band at (3355 cm^{-1}). A spectrum also shows bands at 1633 cm^{-1}, which is a peak similar to graphite and indicates the skeletal vibrations of non-exfoliated graphite, as well as C–O stretching vibrations of epoxy groups 1166 cm^{-1} and alkoxy groups 1040 cm^{-1}.The band indicates the presence of epoxides, and a (FTIR) spectra on GO also showed The reality of existence of asymmetric bands of epoxide at (875 cm^{-1}) and (574 cm^{-1}) OH out-of-plane bend. Consequently, The (FTIR) result verified that the GO structure contained a

range of functional groups that contained oxygen., including hydroxyl, epoxy, carboxyl, and carbonyl[16].

Table 3. The IR Absorption bands characteristic to laser graphene oxide (GO) are assigned.

Wavenumber (cm^{-1})	Functional group	Reference
3355	C–OH stretching vibrationof a hydroxyl group	(Kayode Oladele lumurewa *et al* ., 2017)
1633	C =C stretching vibrations	
1166	C–O elongation of epoxy groups	(I. O. Faniyi *et al* ., 2019)
1040	C–O Alkoxy group stretching	
875	asymmetric epoxide bands	
574	OH out-of-plane bend	

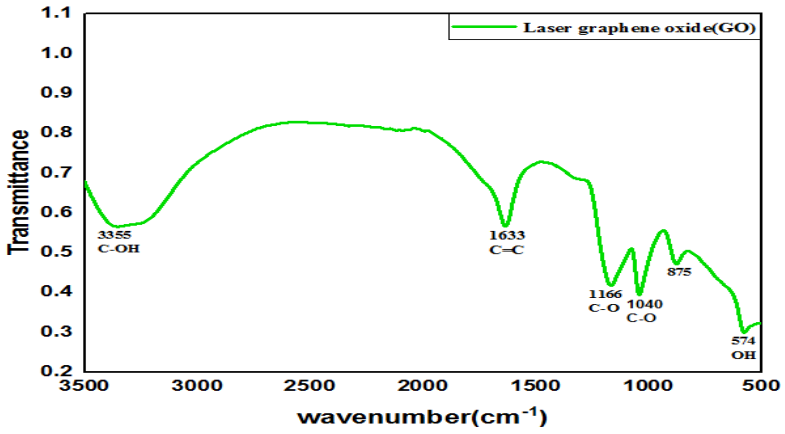

Figure 11: FTIR for Laser graphene oxide (GO)

Raman analysis for Laser graphene oxide (GO)

Sample structural properties graphene oxide were revealed using Raman spectroscopy after preparing them by laser ablation. Where figure (12) demonstrate a strong because the D band is stronger than the G band, the crystal sizes are relatively small. About the D peak location is linked to a structural irregularity like the material's edges or faults. The (G) band peaks at (~1605 cm^{-1}) and the D band at (~1350 cm^{-1}). The G peak represents the (E_2g) phonon from the stretching of carbon sp2 atoms, whereas the (A_1g) symmetric D peak depicts the k-point phonons' breathing mode. A proportion of intensity (ID/IG) between three peaks show how good the content is.

Where strong intensity appear in the D band of the synthesis laser(GO) [17]. Thus, the number of defects is large on its surface ,while The G band of higher intensity of laser(GO) represents a material that is more crystalline . Show that the (ID/IG) (D to G) band intensity ratio) is (0.92). [18]

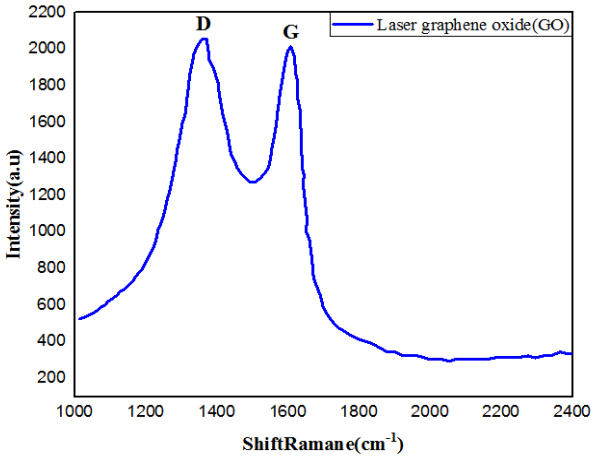

Figure 12 : GO's Raman spectra, produced using several techniques and suggesting the deconvolution of the D and G bands. G (~1605 cm^{-1}), the principal vibrational mode in-plane, and D (1350 cm^{-1}) are the two main peaks produced by GO. another in-plane vibration's second-order overtone

TEM for laser graphene oxide(GO)

Figures (13) shows TEM micrographs and size distributions histogram for GO which range (42-103 ,53-103 and 45-115 nm) prepared by laser energy at 300 mJ

It was observed that GO have a spherical shape form with mean size particles of (66.8,68.8 and 87.7 nm) respectively. Furthermore, the electrostatic

attraction between the nanoparticles causes a notable appearance of GO aggregation in TEM micrographs. Graphite is ablation by pulsed laser, a photo thermal process. The laser pulse raises the target's temperature, which causes material to melt and, in the end, ejects ablated material from the target's surface.

This may cause carbon nanostructure materials (CNMs) to be ejected in the case of graphite. These extremely compact molecules have a strong heat diffusion, which can lead to aggregations, collisions, and the creation of new structures [19].

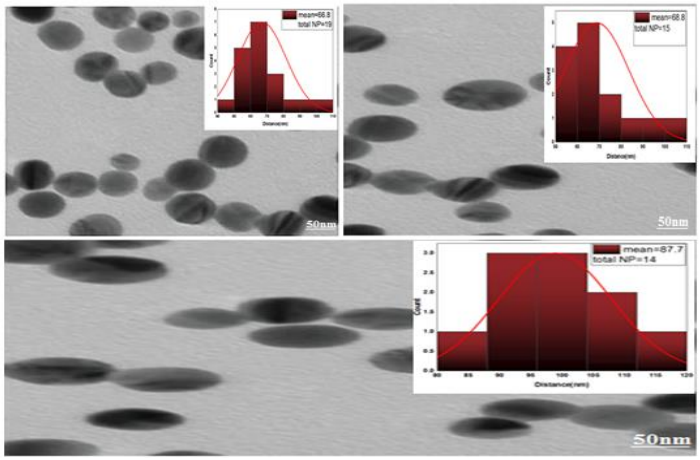

Figures 13. TEM images for laser graphene oxide(GO) and the size distribution histogram with curve of normal-log distribution, mean value

Radiology for the femur

At the conclusion of the second week following surgery, radiographic assessment within the treatment cohort demonstrated early development of new bone and a translucent callus started to form in the afflicted area figure (14). After three and four weeks of surgery, the bony bridge developed in the therapy group. The remodeling phase began at the conclusion of the fifth post-operative a week, and a callus development shrank in opacity and size during a next few a weeks [20]. After the first week of treatment in the group, the process of implanting a scaffold made from a sample laser graphene oxide(GO) demonstrated excellent results through early development of new bone during the initial phase of bone healing, followed by an increase in the amount and opacity within the 2nd and 3th weeks following surgery, as a result of tissue activated osteoblast. By the end of the second week, the new bone production was becoming noticeable, and it increased steadily over the following weeks after surgery, the periosteal reaction often appear radiographically between 5 and 11 days later, with findings mentioning more

abundant and mineralized new bone tissue. Vasodilatation is the cause of the treatment group's mature and full trabecula bone [21]

Histological for the femur

At two week , Only one-third of the bone gap showed signs of new bone growth. figure(15)

After three week post-operative, histological analysis showed an trabecula bone production increased; these bones looked mature, broad, well-mineralized, and had few cavities.

At four week , There were still ingredients for the bone graft. The implant surface was in contact with the newly created, low-density bone figure(15) [22].After the five week post -operative, the control group had mature trabecula bone growth that was wonderfully mineralized, broadening, and creation of lamellar bones that partially encircled the bony apparatus, the have rsian canal's diameter increased as in the blood vessels and osteocytes-filled, empty osteocyte lacuna of the bony device[23]. After conducting physical and mechanical examinations, it was found that the control group exhibited greater density and hardness[24]. Additionally, the control group's fracture tolerance was examined under pressure and heat [25].

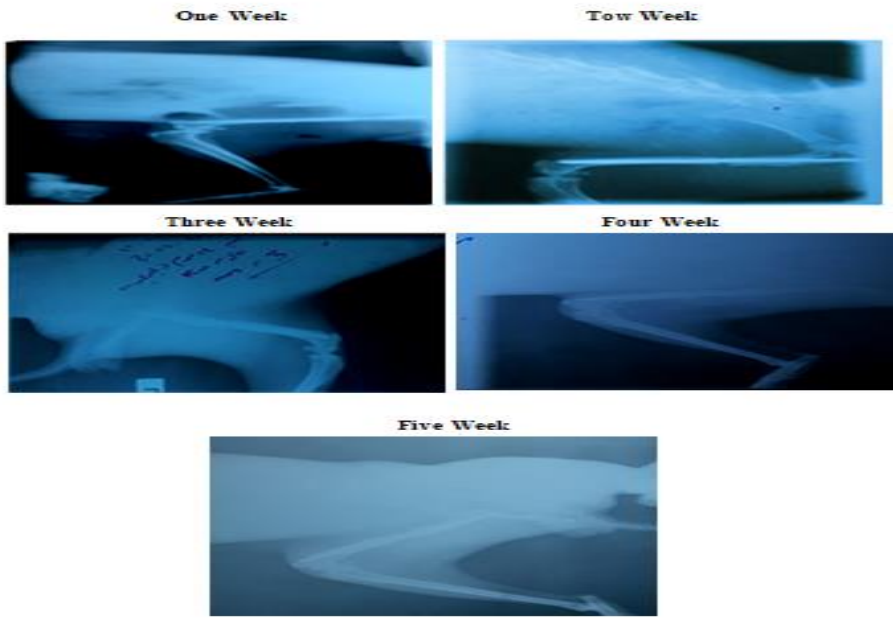

Figures 14: a Radiological finding for control group

مجلة كلية التربية الاساسية
كلية التربية الاساسية – الجامعة المستنصرية
Journal of the College of Basic Education Vol.31 (NO. 129) 2025, pp. 130-147

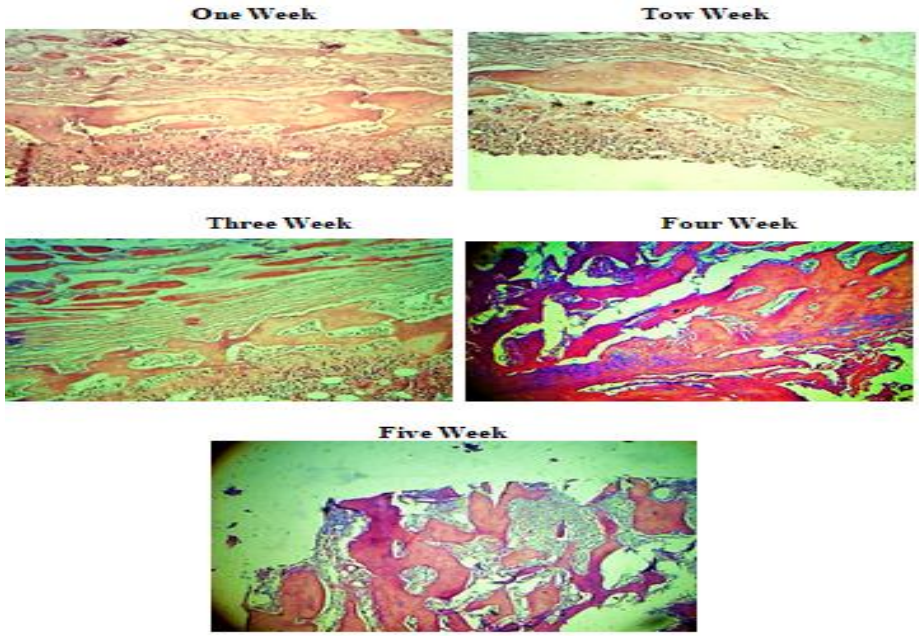

Figure15: a Histological examination of the reference group. H&E. 4

Conclusion:

In this work, we combined (GO : AuNPs) to create composite porous scaffolds using laser ablation.

- the XRD patterns shows two peaks for GO has a distinct characteristics of carbon peak (001). revealed at (2ɵ=10.9°), and the hydroxyl, epoxy, and carboxyl groups present causes a broad diffraction new peak (002) to arise at 2ɵ = 24.9 ° with d-spacing of 8.19 Å. sharp peaks confirmed the high degree of crystallinity of the prepared hexagonal GO phase. The high concentration Using GO groups containing oxygen significantly enhances the mechanical characteristics, according to FTIR scanning data , improving the functioning of the Xeno bone scaffold.

-The results in the Raman spectra indicates the presence of many flaws on the graphene oxide's surface, and therefore its surface is covered with oxygen groups and has edges.

-The results of TEM image analysis showed heterogeneous distribution of spherical particles of different sizes on the graphene oxide surface. Notice that most for that particles are gathered in the center of the surface, and this indicates microscopic peeling of the surface of graphene oxide and Form oxygen groups.

- The GO :AuNPs nanocomposites that were produced demonstrated outstanding biocompatibility, which makes them promising for use as implants and thus promote bone formation and regeneration.
-Histopathological examinations showed that implantation of the (GO: AuNPs) scaffolds contributed in the formation of new bone by further improving the physical properties, such as protein and calcium uptake, enzyme resistance, and compressive strength. The purpose of this study is to create composite components that can effectively mend bone defects

References

1.Cheng, J., et al., Two-dimensional black phosphorus nanomaterials: emerging advances in electrochemical energy storage science. Nano-micro letters, 2020. 12: p. 1-34.
2.Pykal, M., et al., Modelling of graphene functionalization. Physical Chemistry Chemical Physics, 2016.vol18(9): p. 6351-6372.
3.Li, A., C. Zhang, and Y.-F. Zhang, Thermal conductivity of graphene-polymer composites: Mechanisms, properties, and applications. Polymers, 2017. vol 9(9): p. 437.
4.Mohanraj, J., D. Durgalakshmi, and A. Rakkesh, Current trends in disposable graphene-based printed electrode for electrochemical biosensors. Journal of The Electrochemical Society, 2020. vol 167(6): p. 067523.
5.Song, C., et al., Study on AgInZnS-graphene oxide non-toxic quantum dots for biomedical sensing. Frontiers in Chemistry, 2020. vol 8: p. 331.
6.Xu, Z., et al., Ultrastrong fibers assembled from giant graphene oxide sheets. Advanced Materials, 2013. Vol 25(2): p. 188-193.
7.Wright, Z., et al., Functional graphenic materials, graphene oxide, and graphene as scaffolds for bone regeneration. Regenerative Engineering and Translational Medicine, 2019.vol 5: p. 190-209.
8.Biru, E.I., et al., Graphene oxide–protein-based scaffolds for tissue engineering: recent advances and applications. Polymers, 2022.vol 14(5): p. 1032.
9.Shuai, Y., C. Mao, and M. Yang, Protein nanofibril assemblies templated by graphene oxide nanosheets accelerate early cell adhesion and induce osteogenic differentiation of human mesenchymal stem cells. ACS applied materials & interfaces, 2018.vol 10(38): p. 31988-31997.
10.Cheng, C., et al., Functional graphene nanomaterials based architectures: biointeractions, fabrications, and emerging biological applications. Chemical reviews, 2017.vol 117(3): p. 1826-1914.
11.12. Vial, S., R.L. Reis, and J.M. Oliveira, Recent advances using gold nanoparticles as a promising multimodal tool for tissue engineering and regenerative medicine. Current Opinion in Solid State and Materials Science, 2017.vol 21(2): p. 92-112.

12.Bozorgi, A., et al., Application of nanoparticles in bone tissue engineering; a review on the molecular mechanisms driving osteogenesis. Biomaterials science, 2021. Vol 9(13): p. 4541-4567.
13. Frens G, Controlled nucleation for the regulation of the particle size in monodisperse gold suspensions, Nature Physical Science, 241 (1973) 20–22. DOI: 10.1038/physci241020a0
14.Gaidukevic, J., et al., A novel approach to prepare highly oxidized graphene oxide: structural and electrochemical investigations. Applied Surface Science, 2021.vol 567: p. 150883.
15.Nien, Y.-H., et al., Preparation of a Novel Nanostructured Lead Titanate Composite Photocatalyst and Its Degradation of Organic Dyes under Visible Light. Journal of Composites Science, 2023.vol 7(10): p. 434.
16.Muhsan, A.A. and K. Lafdi, Numerical study of the electrochemical exfoliation of graphite. SN Applied Sciences, 2019. Vol 1: p. 1-8.
17.Marcin Behunová, D., et al., Electrophoretic deposition of graphene oxide on stainless steel substrate. Nanomaterials, 2021.vol 11(7): p. 1779.
18.Olumurewa, K.O., et al., Characterization of high yield graphene oxide synthesized by simplified hummers method. Graphene, 2017. vol 6(4): p. 85-98.
19.Lin, T., et al., Laser-ablation production of graphene oxide nanostructures: from ribbons to quantum dots. Nanoscale, 2015.vol 7(6): p. 2708-2715.
20.Hassan, M.A.M., A.M. Abbas, and M.J.M. Ali. Construction of Scaffold from MgO nanoparticle: bone fracture healing. in IOP Conference Series: Materials Science and Engineering. 2020. IOP Publishing.
21.Shi, H., et al., Hydroxyapatite based materials for bone tissue engineering: A brief and comprehensive introduction. Crystals, 2021. vol 11(2): p. 149.
22.Peng, W., et al., The healing effect of platelet-rich plasma on xenograft in peri-implant bone defects in rabbits. Maxillofacial plastic and reconstructive surgery, 2016. vol 38: p. 1-9.
23. Magda Silva, Isabel S. Pinho, José A. Covas, Natália M. Alves and Maria C. Paiva, 3D printing of graphene-based polymeric nanocomposites for biomedical applications, Functional Composite Materials (2021).
24.Hassan, M.A.M., A.H. Mohammed, and Z.K. Hamzh, Potential Role of Laser Therapy on Scaffold Implantation for Osteogenesis and Regeneration with Microbial Protection. BioNanoScience, 2022. vol 12(4): p. 1059-1085.
25. Junyao Cheng, Jianheng Liu, Bing Wu, Zhongyang Liu, Ming Li , Xing Wang, Peifu Tang and Zheng Wang1, Graphene and its Derivatives for Bone Tissue Engineering: In Vitro and In Vivo Evaluation of Graphene-Based Scaffolds, Membranes and Coatings ,Frontiers in Bioengineering and Biotechnology ,September 2021 , Volume 9.

مجلة كلية التربية الاساسية
كلية التربية الاساسية – الجامعة المستنصرية
Journal of the College of Basic Education Vol.31 (NO. 129) 2025, pp. 130-147

اصلاح عيوب عظم الفخذ لدى الأرانب باستخدام هياكل أكسيد الجرافين وجزيئات الذهب النانوية

وهب باسم مهدي1، هاجر تونسي قرمازي2
1قسم الفيزياء، كلية العلوم، الجامعة المستنصرية، بغداد، العراق
2قسم الفيزياء، كلية العلوم بصفاقس، جامعة صفاقس، تونس
موبايل:07750777599
موبايل:92019819

مستخلص البحث :
الخلفية: المنتج الثانوي لأكسدة الجرافيت هو أكسيد الجرافين، والذي يوفر فرصة هائلة لتطوير مجال الطب التجديدي بشكل كبير. نظرًا للصفات المواتية لأكسيد الجرافين - بسبب صفاته الميكانيكية القابلة للتكيف والتوافق البيولوجي وقابلية التحلل. الهدف: يهدف هذا البحث إلى توظيف أشعة الليزر لاستئصال سطح الجرافيت وتحضير أكسيد الجرافين بخواص ميكانيكية ممتازة تساهم في علاج إصابات عظام الأرانب وتجديد أنسجة العظام التالفة والتمايز العظمي. الطرق: في هذا العمل، تم تحضير زراعة هياكل عظمية زينو في جزأين فيزيائيًا: تم توليد أكسيد الجرافين (GO) بفعالية باستخدام تقنية الاستئصال بالليزر. مدة نبضة الليزر (1064 نانومتر) مع طاقة الليزر (300 مللي جول)، بعد ذلك، تم تحميل جسيمات النانو الذهبية (AuNPs) المحضرة مسبقًا على سطح أكسيد الجرافين باستخدام طريقة الرقائق. تم فحص بنية ومورفولوجيا المركب (GO: AuNPs) باستخدام مطيافية تحويل فورييه بالأشعة تحت الحمراء (FTIR) وحيود الأشعة السينية .(XRD) باستخدام مطيافية رامان والمجهر الإلكتروني النافذ(TEM) ، تم التحقيق في اتجاهات حافة أكسيد الجرافين / البلورية وترتيب التكديس بيولوجيًا: في هذا القسم، تم وصف تقنية تحضير قالب دبوس لترسيخ زرع السقالة في كسور عظام الفخذ المحفزة للأرانب. تم استخدام مزيج مصنوع من أكسيد الجرافين وجسيمات النانو الذهبية لإنشاء سقالة عظمية زينو. النتائج: أظهرت النتائج النسيجية في الجسم الحي للموقع المعالج بسقالات(GO: AuNP) ، التي تم حصادها في الأسبوع الأول بعد التطعيم، تمعدن العظام وتكوين عظام جديدة وفيرة دون أي علامة على وجود التهاب في مجموعة العلاج. علاوة على ذلك، أظهرت الاختبارات المختبرية أن سقالات (GO: AuNP) تعزز بشكل كبير خلايا التصاق الخلايا العظمية وكذلك النمو. الاستنتاج: حول تطبيق أكسيد الجرافين (GO) لتعزيز امتصاص الكالسيوم والبروتين ومقاومة الإنزيمات والقوة البدنية.

الكلمات المفتاحية: أكسيد الجرافين؛ جسيمات النانو الذهبية؛ سقالة عظمية زينو؛ الاستئصال بالليزر؛ عظم الفخذ.
ملاحظة: البحث مستل من أطروحة الدكتوراه.